ELSEVIER

Beam tests of prototype fiber detectors for the H1 forward proton spectrometer

J. Bähr, K. Hiller*, B. Hoffmann, H. Lüdecke, A. Menchikov, R. Nahnhauer,
H.E. Roloff[†], F. Tonisch, R. Völkert

Deutsches Elektronen-Synchrotron DESY, Institut für Hochenergiephysik IfH, Zeuthen, Germany

Received 19 June 1995

Abstract

Different prototypes of fiber detectors with an internal trigger system were tested in a 5 GeV electron beam at DESY. A silicon microstrip telescope was used for an external reference measurement of the beam to study the spatial resolution of the fiber detectors. On average 75% of all crossing electron tracks could be reconstructed with a precision better than 150 μm. These successful methodical investigations led to the installation of similar detectors in the proton beamline 81 m downstream of the central H1-detector at HERA as part of a forward proton spectrometer in spring 1994.

1. Introduction

In the upgrade program of the H1 experiment at HERA the construction of a forward proton spectrometer (FPS) is proposed [1]. Its aim is to measure the trajectories of high-momentum particles which escape the central H1 detector through the beam pipe. The FPS consists of precise tracking detectors installed in movable vacuum inserts (Roman Pots) in the proton beam line downstream H1. Since the deviation of these particles from the nominal beam profile is only a few millimeters a high spatial resolution is necessary to reach a reasonable momentum resolution. Another important parameter of the Roman Pot detectors is a short response time which fits to the 96 ns bunch crossing time of HERA. First hints on diffractive processes in ep-scattering have been reported by ZEUS [2] and H1 [3]. Events with large rapidity gaps indicating one or more missing particles in the forward direction were found [4]. The FPS allows the registration of such high momentum particles.

The ZEUS experiment has completed the installation of a leading proton spectrometer based on silicon micro strip detectors, and first data were collected. The FPS project of H1 foresees tracking detectors of scintillating fibers read out by position sensitive photomultipliers (PSPM). In the first phase of the H1 project two Roman Pots (RP) at the positions 81 m and 90 m downstream from the H1 central detector will be equipped with two separated fiber detectors [5] which measure the particle trajectories with a

precision of about 100 μm. The measurement of two space points would already give a rough direction of track candidates allowing the suppression of several background sources. Monte Carlo simulations have shown that a sensitive detector size of about $3 \times 6 \text{ cm}^2$ is sufficient to measure scattered protons with momenta above 400 GeV with an acceptable efficiency.

The aim of the test run was to measure the resolution and the efficiency of the fiber detectors as well as the functionality of all of their components. Different scintillator materials and fiber mappings on the PSPM photocathode were tested. The two detectors of 1 mm scintillating fibers were read out via spliced light guide fibers by two PSPMs H4139-20[1]. All geometrical parameters were chosen as close as possible to the future arrangement in the Roman Pots.

2. The setup

The test setup consists of three essential parts: the fiber detectors including their readout via PSPM and their internal trigger counters, the external trigger system and the silicon microstrip detectors (MSD) used for an independent measurement of the beam tracks.

A schematical view of all components is shown in Fig. 1. A detailed description of the fiber detectors follows in the next section. The external trigger system consists of

_____

* Corresponding author. E-mail: hiller@ifh.de.
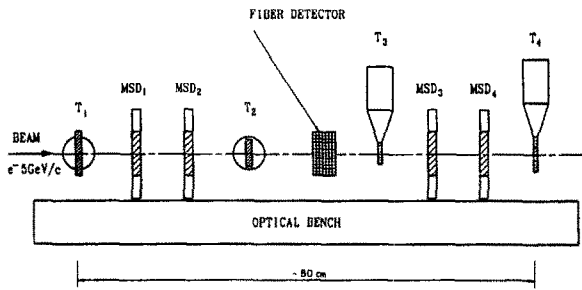[†] Deceased.

Fig. 1. The experimental setup. The scintillation counters of the external trigger system are denoted by T1–T4, the positions of the four silicon microstrip paddles are indicated by MSD1–MSD4.
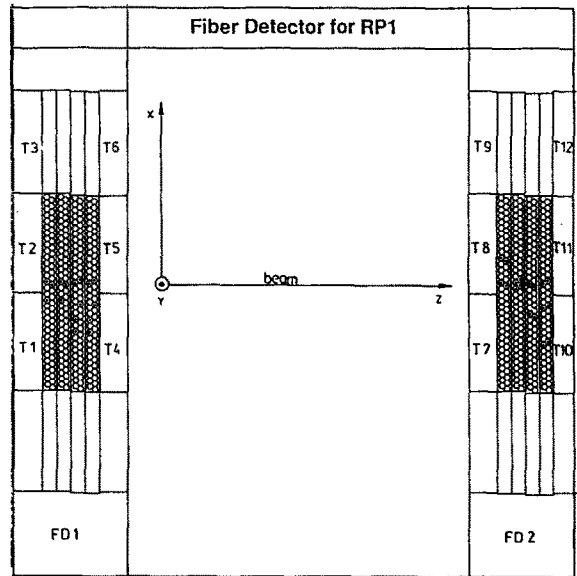

Fig. 2. Layout of the Roman Pot fiber detectors. The two subdetectors FD1 and FD2 are shown together with a measured hit pattern response indicating a traversing particle and some noise hits. The coordinate system is indicated between the two subdetectors, and the positions of the segments T1–T12 of the internal trigger system are given.

four scintillation counters in front of and behind the fiber detectors read out by XP1911 photomultipliers[2]. The two outer counters have a sensitive area of 3×3 cm^2 each, the inner counters of 1×3 cm^2 are arranged in crossed geometry. The coincidence of their signals was used to trigger the readout of the fiber detectors and the MSDs.

The MSD telescope was already used in previous beam tests [6]. It measures the coordinates of the beam particles to ensure a reliable calculation of the efficiency and the spatial resolution of the fiber detectors. It consists of four paddels oriented perpendicular to the beam direction. The common sensitive area of the paddle covers about 3×3 cm^2. The readout pitch of all paddles is 100 μm which results in a measurement precision per crossing particle of about 25 μm.

The data acquisition was performed by an OS/9-system controlling the VME and CAMAC readout modules [7].

2.1. The fiber detector prototype

A fiber detector prototype consists of two subdetectors FD1 and FD2 which are separated by a distance of 70 mm. To obtain a better spatial resolution they were staggered by 65 μm. The layout of the fiber detector is sketched in Fig. 2. The fibers of FD1 and FD2 are read out by two PSPMs with 64 channels each. The application of this type of PSPM for fiber readout is described in Ref. [7].

Every subdetector has 4 double layers of two times 32 fibers of 1 mm diameter and 1.05 mm pitch, internally staggered by 500 μm. The third and fourth double layers are staggered by 250 μm to the first and second one. In total there are 256 fibers to be mapped to 64 PSPM pixels which correspond to a fourfold multiplexing (see Section 2.2).

Each single fiber consists of a 3 cm scintillating part thermally spliced to a light guide of about 45 cm length. To test different fiber materials we produced FD1/FD2 both from POLHITECH-fibers (RP3A/B, respectively)

and from BICRON-fibers (RP5A/B, respectively) [5]. To measure the efficiency of a single fiber layer we used in a few special runs only the double layers 2 and 3 of RP3A which form a detector of four single layers with 250 μm regular staggering (compare Fig. 3a). In the following we call it RP3A/2.

As illustration Fig. 2 shows a measured hit pattern at the fiber detector end faces. Hits from the crossing particle as well as background hits are marked. The different hit pattern of FD1 and FD2 results from the different multiplexing schemes of the fibers to the 8×8-pixel array of the PSPM.

2.2. The multiplexing schemes

The different mapping schemes for FD1 and FD2 are illustrated in Figs. 3a and 3b, respectively. The four fibers put to one PSPM-pixel are marked by the same number. In the text we will refer to these mappings as A- and B-type detectors (masks), respectively. Whereas the first assembly ensures a high single hit efficiency by doubling the fiber material for a traversing particle, the last one was designed to avoid dead regions between two fibers. In Figs. 3a and 3b we illustrate the influence of these two kinds of mapping on the hit pattern of a crossing particle, marking all fibers assigned to the track. If one of the four fibers mapped to a PSPM-pixel has a signal above a defined threshold (see Section 3), all four fibers have to be treated as hit candidates. It is easy to see that this results for mask
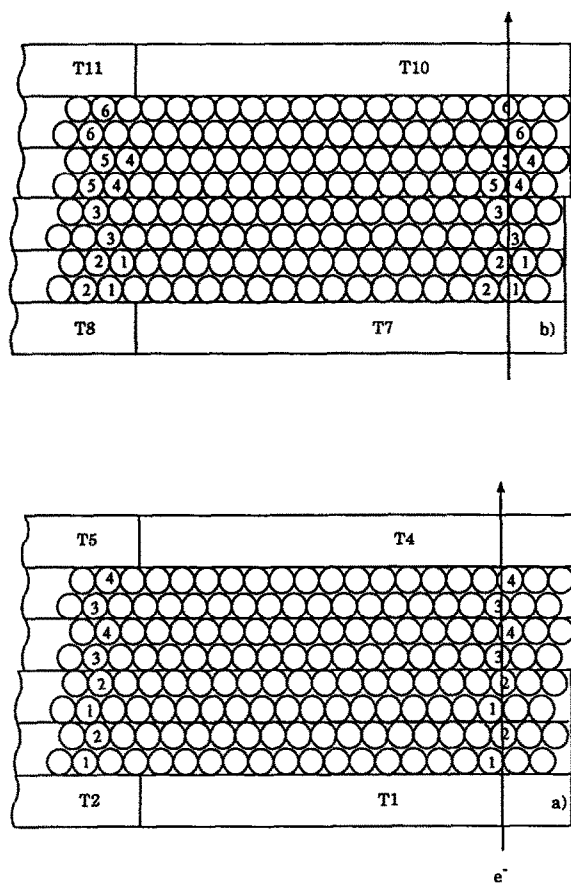
Fig. 3. Illustration of fiber mapping to PSPM pixels. (a) and (b) show the mapping for the masks A/B, respectively. The different response to a traversing particle is shown. All fibers coupled to one PSPM channel are marked with the same number. The segments of the internal trigger system to resolve the coordinate multiplexing (e.g. signals in T1/T4 or T2/T5) are also shown.

A in a doubling of the number of hit fibers, whereas for mask B on the average three times as many fibers are indicated as were crossed. Since two fibers of two single layers staggered by 500 μm were put to the same PSPM pixel we get in this case an effective fiber diameter of 1.5 mm which will influence the obtainable resolution (see Section 5). For A-type detectors the effective fiber diameter equals to the fiber diameter of 1 mm since the x-position of two fibers is identical.

2.3. The internal trigger system

It can also be seen in Fig. 3 that fiber numbers different by 16 are connected to one PSPM pixel. This regular multiplexing has to be resolved using the information from the segmented internal trigger system which is also sketched in Figs. 2 and 3. These segments are made of 5 mm thick scintillating plates with imbedded wavelength shifter fibers to be read out separately by photomultipliers

XP1911. It was one of the aims of this test run to find out whether it is possible to resolve the coordinate ambiguities by such a trigger system.

2.4. A non prototype fiber detector

The regular multiplexing scheme of the A- and B-masks generates the so-called ghost hits which can be excluded by the described segmented trigger system. To avoid the additional material of the internal triggers in future applications we built a special detector of 8 single layers of BICRON fibers using a mask with a stochastic multiplex scheme. Coupling 7 fibers to each PSPM-readout channel it was possible to enlarge the number of fibers per layer from 32 to 56. Except the detector width all geometrical parameters of this detector are the same as for those with masks A and B. In the following we denote that detector as RP4 and the stochastic fiber mapping as the MUX-mask.

3. The data analysis

The following analysis is based on about 40 000 events with informations from the MSD telescope as reference system. The data set of each event consists of three parts: the two times 8×8 PSPM amplitudes for the fiber detectors, the 12 amplitudes of the internal trigger system and the 12×320 amplitudes of the MSD telescope. For each of these data parts we determined the pedestals, as well as other necessary calibration data.

A sensitivity table has been measured for each PSPM coupling a light emitting diode (LED) via a 1 mm fiber to the center of every PSPM pixel. The LED light output was calibrated to the light produced by a minimum ionizing particle traversing a 1 mm scintillating fiber. The pixel sensitivities vary by about a factor 2 for both devices.

3.1. The fiber detector data

In a first step of the data analysis the relative pixel sensitivities are used to correct the pedestal subtracted PSPM amplitudes.

To decide which PSPM pixel corresponds to a hit fiber we accepted all amplitudes above a threshold which is about 5 standard deviations of the pedestal distribution. From earlier studies [7] we know that there is some noise randomly distributed over the PSPM surface and a low rate of cross talk mainly into the neighbouring PSPM channels. To find the hit fiber we searched for local amplitude maxima on the PSPM anode pixel matrix. This procedure reduces the background from neighbouring fibers especially for mask A.

For the MUX-mask with the RP4 detector one expects a larger number of fiber hit candidates due to the higher multiplex factor. For that detector we accepted all PSPM

pixels with amplitude above the threshold not to loose signals.

All fibers mapped to an accepted PSPM pixel were marked as fiber hit candidates for the following algorithm. It takes advantage of the fact that particle tracks cross the fiber detectors mainly perpendicular to the fiber planes. The coordinate range of a traversing particle is given by the overlapping region (corridor) of all hit fibers. A track point candidate was accepted if the number of hits in this corridor exceeds 3 for detectors with the A- and B-mask and 5 for the RP4 detector with the MUX-mask. The best estimation of the x-coordinate of the track point is the center of the corridor. The corresponding z-coordinate was fixed to be the middle z-position of the subdetector, the y-coordinate was not measured.

Since there were two subdetectors, we could check their orientation to the beam. For all combinations of tracks points in FD1 and FD2 we calculated the slope of their connecting line. The narrow width of the resulting angular distribution allows the removal of wrong combinations. Since the detectors are staggered to each other the measuring accuracy of a combined final track point is better than that one of a single detector due to the reduced common corridor. To take advantage of this fact one has to know the external alignment of the fiber subdetectors to the beam with a high precision which does not hold good for our experimental setup. So we gave as final track point coordinates the arithmetical means and as resolution the higher precision of the included track points from the FD1 and FD2 measurements.

3.2. The internal trigger system

The measured amplitudes of the segmented trigger system for FD1 are shown as example in Fig. 4 for a narrow beam width of about 1.5 cm adjusted to the second half of the fiber detectors (see Fig. 2). That means we expect track signals mainly in T2 and T5. It can be seen that the amplitudes of these segments differ significantly from the others, allowing a clear resolution of the regular coordinate multiplexing.

The internal triggers have a detection efficiency of about 98% of the external trigger system. Correspondingly about 96% efficiency is found for that beam position by requiring a twofold coincidence.

3.3. The MSD data

For the analysis of the MSD data we used two independent methods. The first one is an iterative procedure using only MSD data to align the MSD paddles. The second one uses the reconstructed track points in FD1 and FD2 to adjust the MSD data to the fiber detector coordinate system. Both obtain similar track residuals of about 35 μm and track efficiencies of about 55% and 25% for MSD tracks with three and four hits per track, respectively.
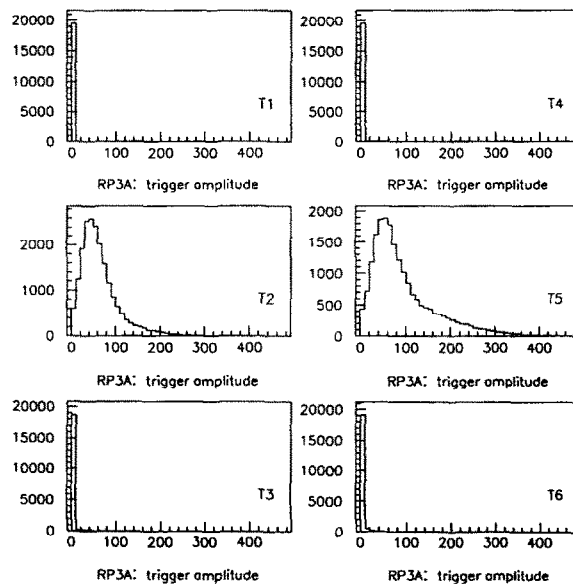

Fig. 4. Amplitude distributions of the internal trigger system arranged in the form of three scintillator tiles in front of (T1, T2, T3) and behind (T4, T5, T6) each fiber detector.

For the determination of the efficiencies of the fiber detectors we used the event sample which have a reconstructed beam in at least three MSD paddles. For the study of the fiber detector spatial resolution, only events with a track based on hits in all four MSD paddles were used to minimize the influence of the MSD reconstruction error.

4. Detector efficiency

A basic quantity of a multilayer fiber detector for coordinate measurements is its detection efficiency for traversing particles. Fig. 5 shows all fiber hits of the RP3A detector near to the beam track which is reconstructed by the MSD telescope. Theoretically, the maximum distance of any fiber hit from the track should be the half of the fiber diameter. As we can see in Fig. 5, the most fiber hits are near to the beam track, but there are still hits outside the theoretical corridor, and also a significant contribution of uncorrelated background hits can be observed.

The reason for track related hits outside the theoretical corridor can be physical processes like the appearance of low energetic delta-electrons around the traversing particle, deviations from the ideal detector geometry and the above mentioned PSPM noise. To obtain the correct value of the efficiency we enlarged the maximum distance of track hits from the reconstructed track point to 1 mm for detectors with the A-mask/MUX-mask and to 1.5 mm for detectors with the B-mask. The contribution of background hits was estimated in a region far from the beam track. It was subtracted from the hits in the track corridor and the
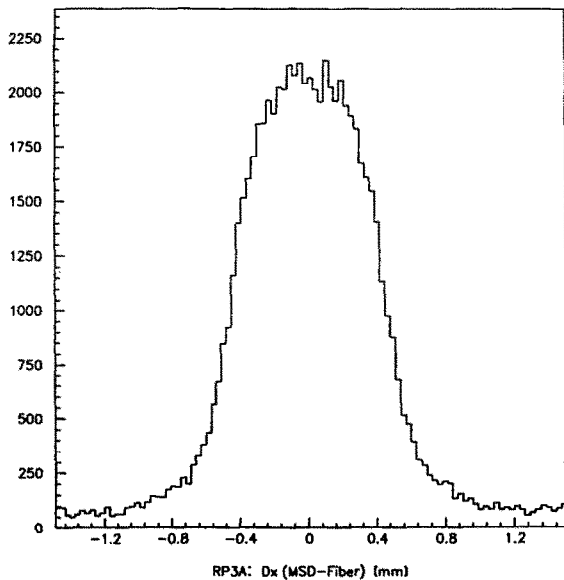
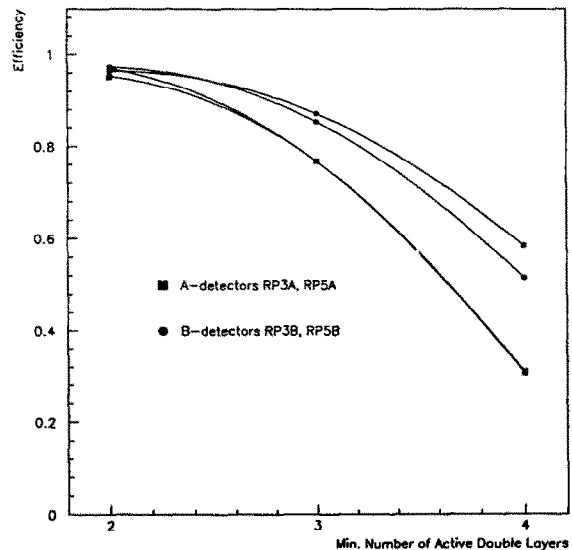Fig. 5. Difference of x-coordinates of all fiber hits to the MSD prediction for the RP3A-detector.

Fig. 6. Efficiency to reconstruct a track point in dependence on the number of active fiber double layers per track for the detectors RP3 and RP5.

resulting efficiencies are quoted in Table 1. For detectors with the A- and the B-mask the fibers of two single layers are multiplexed to the same PSPM channels and the average efficiency per double layer is given. Since the fibers of the RP4 detector are stochastically multiplexed, the average efficiency is quoted per single fiber layer.

The detectors with the A-mask have an average efficiency per double layer of about 70% while the corresponding values for detectors with the B-masks are about 75%, slightly larger. All efficiencies of the individual layers differ less than 10% from the quoted values in Table 1. The RP3B detector was measured in three separate run periods and the resulting efficiencies differ by about 1%. By mechanical reasons detectors with the A- and B-mask could never be coupled to the same PSPM and their efficiencies are influenced by the different PSPM qualities.

The single fiber layer efficiency as measured by the detectors RP3A/2 and RP4 is about 60%. A comparison with the corresponding efficiency values of the double layers indicates that in most cases a double layer of 1 mm fibers will not much improve the detection efficiency for minimum ionizing particles.

The efficiency for the detection of particles in depen-

Table 1
Average efficiency per double/single (*) fiber layer

Detector	Efficiency [%]
RP3A	68
RP3B	78
RP3A/2(*)	62
RP4/MUX(*)	58
RP5A	69
RP5B	74

dence on the minimum number of fiber hits in the double layers is shown in Fig. 6 for detectors with the A- and the B-mask. As one expects, the efficiency is near to 100% requiring only two active double layers. It decreases to about 75% for detectors with the A-mask and 85% for those with th B-mask for crossing tracks with at least three active double layers. Again the efficiency of detectors with the B-mask is superior to the A-mask detectors. The detector with the MUX-mask has some peculiarities which influence the track point reconstruction. The stochastic multiplexing generates a non-negligible fraction of ghost track points which is shown in Fig. 7 together with the efficiency of the RP4 detector in dependence on the number of hits in the single fiber layers. The efficiency decreases steadily from about 90% for at least four hits to about 10% requiring hits in all 8 layers. For a minimum number of five hits the efficiency is 83% and the average number of additionally 1.3 ghost track points per event appear in the reconstruction. The decision which track points are ghosts is done using the MSD informations.

Finally the probability of reconstructing a track point in both subdetectors FD1 and FD2 is about 70% for at least three hits in the double layers of RP3/RP5 or five hits in the single layers of the RP4. This relatively low value for the efficiency is influenced by the strong selection criteria and the fact that the two subdetectors are treated independently. In the case of a well known alignment of the fiber detectors to the beam one can use the hits from both subdetectors to decide for a crossed track which increases the efficiency significantly. We calculate 98% or 94% efficiency to detect a crossing particle if we require fiber hits in at least 3 or 4 from the 8 double layers, respectively.
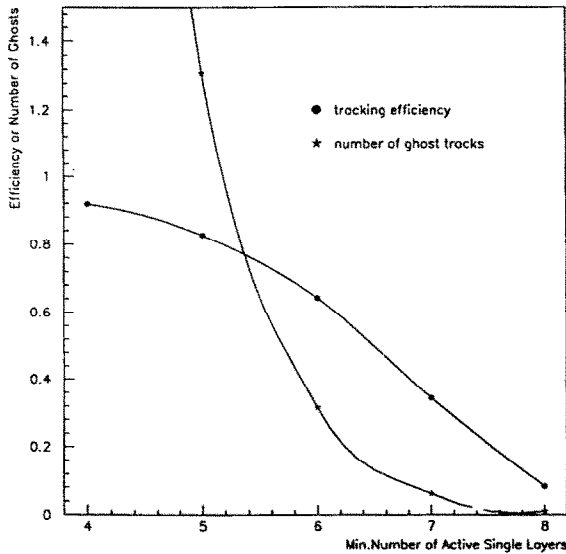
Fig. 7. As Fig. 6 but for the RP4-detector for single layers. Additionally the number of reconstructed ghost tracks due to the stochastic multiplexing is given.
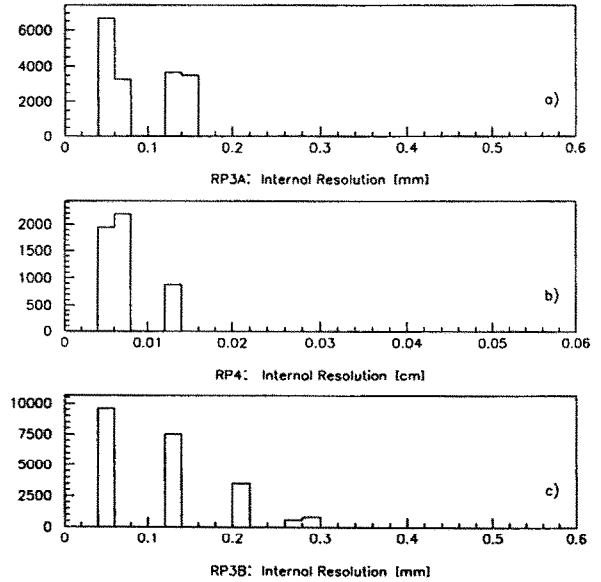

Fig. 8. (a)–(c) Internal resolution for the detectors RP3A, RP4 and RP3B, respectively. The digitized form results from the different combinations of overlapping fibers.

One should keep in mind that all quoted values of efficiencies do not only reflect the quality of the fiber detector but take into account also the inefficiencies of the PSPMs and of the subsequent readout chain.

5. Detector resolution

Assuming an ideal detector geometry the minimum possible overlap of fibers of different layers is 200 μm. This leads to a position measurement error of about 60 μm. This value will be modified in dependence on the real fiber efficiency. The number of overlapping fibers decreases and the corridor may become larger. The combinatorics of overlapping fibers results in the digitized distributions of the detector resolution as shown in Figs. 8a–8c for the detectors RP3A, RP4 and RP3B. At least three hits per detector were required. As one can see, detectors with A- and MUX-masks have a slightly better resolution than the B-type detectors as consequence of their smaller effective fiber diameters, see Section 2.2.

Calculating the results given in Fig. 8 we have assumed an exact mechanical precision of the fiber alignment in the detectors. However background hits due to interactions of particles within the detector, multiple scattering or noise from the readout chain may influence the measurement precision. To study these effects we use the independent reference measurement of particle tracks performed with the MSD hodoscope.

In Figs. 9a–9c we show the distributions of the differences between the MSD track prediction and the reconstructed track coordinates in the fiber detectors RP3A, RP4

and RP3B. We fitted the distributions by a Gaussian superimposed by a flat background. The standard deviation of about 150 μm and 200 μm is a rough estimation of the resolution for A- and B-type detectors, respectively. But
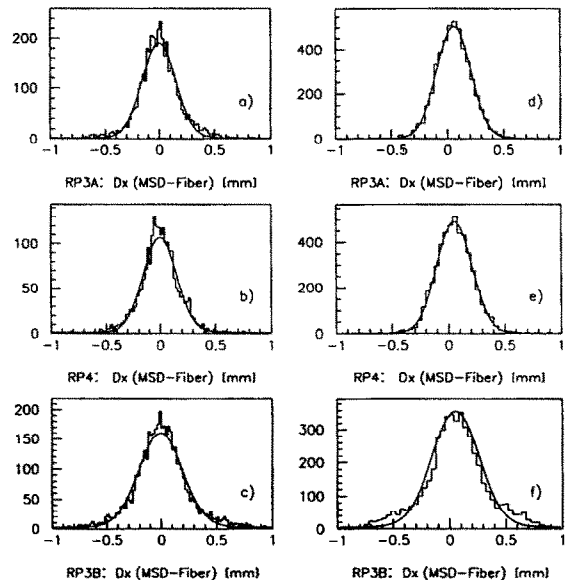

Fig. 9. (a)–(c) Difference of the reconstructed fiber x-coordinates in the fiber detector to the MSD prediction for the detectors RP3A, RP4 and RP3B. (d)–(f): Monte Carlo predictions for the results in (a)–(c). In the Monte Carlo calculations a beam as measured in the test run, 10% background hits and a 2° inclination of the fiber coordinate system to the MSD system are included.

Table 2
Standard deviations and root-mean-square of the fiber detector resolution for all detectors

Detector	Resolution: Data			
	A- and MUX mask		B-mask	
	$\sigma/\mu m$	rsm/μm	$\sigma/\mu m$	rms/μm
RP3	154	202	200	258
RP4	151	193	–	–
RP5	151	195	185	253

the Gaussians show systematic deviations from the data at the tails of the distributions, in particular for B-type detectors. Therefore the root-mean-square (rms) may be the more correct estimation of the resolution. We summarized in Table 2 the standard deviation σ and the rms values for all detectors.

Discussing these results one has to keep in mind the different influence of multiple scattering effects on the MSD track fit and the track point reconstruction in the fiber detectors. Since the fiber detectors are relatively close to each other the effect of multiple scattering is small compared to the MSDs. We made a Monte Carlo simulation of the complete experimental setup using a beam of 5 GeV electrons as measured in the testbeam [8]. Fiber efficiencies are applied in accordance to the measured values. To take care about the noise of the optoelectronic readout, which is concentrated near to the hit fibers [7] we added a corresponding fraction of background hits in this region. Finally we allow a small rotation of the MSD coordinate system w.r.t. the fiber detector coordinate system in the x/y-plane. The real value of the rotation angle α is difficult to estimate because the fiber detectors do not give the possibility of a direct y-measurement up to now. Therefore we varied α in the range 0–5°.

The results of the Monte Carlo simulations are presented in Table 3 for 0%, 5% and 10% noise hits and applying additionally to the 10% noise hits a rotation with $\alpha = 2°$.

For the last case we show in Figs. 9d–9f the Monte Carlo distributions corresponding to the data in Figs. 9a–9c. As one can see the Monte Carlo results with 10% background hits and a rotation of 2° agree with the data rather well. A- and B-type detectors behave quite different with respect to the influence of background hits. For A-type detectors this influence is negligible while the influence is remarkable for B-type detectors. This is due to the multiplexing scheme and the reconstruction procedure of overlapping fibers which increase the probability to include noise hits. Together with the physical noise from interactions in FD1 this results in a broadening of the resolution distribution of B-detectors in comparison to A-type ones.

An additional effect which influences the detector resolution is the inhomogeneity of the arrangement of the fibers over the whole detector area. Cutting a test detector in several pieces this value has been measured to be about 50 μm [5]. Our results on the resolution are compatible with such a value for all detectors.

6. Summary

Several prototype fiber detectors foreseen for use in the H1 forward proton spectrometer run in 1994 have been tested in a 5 GeV electron beam at DESY.

The detectors consist of two times eight fiber layers separated by 7 cm along the beam direction. They allow the reconstruction of one coordinate at two space points of the particle trajectory. The slope of the trajectory through the two detectors can be used to exclude background tracks by an angular cut. Different arrangements of fibers with respect to the optoelectronical readout done by two position sensitive photomultipliers have been tested, combining layers to double layers or using stochastic higher order fiber multiplexing. The probability of an independent reconstruction of a particle track point in both detector parts was found to be about 70% demanding three hits per detector or five hits for stochastic multiplexing. Using both parts in common we reach an efficiency of 98%.

Comparing with an independent reference measurement from a silicon microstrip detector hodoscope we observe a resolution of about 150 μm for simple fourfold double layer staggering and stochastic multiplexing whereas a more complicated fiber arrangement with higher global efficiency but larger noise sensitivity reduces the resolution to about 200 μm. These values include however the uncertainties in the relative alignment of both MSD and fiber detectors for this test run.

Taking into account the possible improvements of the detector alignment for the data taking in Roman Pots it is possible to combine the tracking informations of both detector parts for the reconstruction of the coordinate of a traversing particle. This will improve the efficiency and resolution considerably.

Table 3
As Table 2, for a Monte Carlo simulation of the test experiment. The calculations were done for 0%, 5%, 10% background hits, respectively and 10% background hits with an additional rotation of 2° between the fiber- and the MSD-coordinate systems

Noise hits [%]	Resolution: Monte Carlo			
	A- and MUX mask		B-mask	
	$\sigma/\mu m$	rms/μm	$\sigma/\mu m$	rms/μm
0	121	155	148	186
5	121	165	169	219
10	124	154	179	240
10 + 2° rotation	146	174	195	249

J. Bähr et al. / Nucl. Instr. and Meth. in Phys. Res. A 371 (1996) 380–387

387

References

[1] Letter of interest for a forward proton spectrometer for H1, DESY (1992).
[2] M. Derrick et al. (ZEUS Collaboration), Phys. Lett. B 315 (1993) 481.
[3] H1 Collaboration, DESY 93-087.
[4] M. Derrick et al., Phys. Lett. B (1988) 481.
[5] J. Bähr et al., DESY 93-200.
[6] J. Bähr et al., Nucl. Instr. and Meth. A 324 (1993) 145.
[7] J. Bähr et al., DESY 93-201.
[8] GEANT, Detector Description and Simulation Tool, CERN (193).